DOI: 10.19884/j.1672-5220.202411009

Gray Fabric Defect Detection Based on Statistical Template Matching

LI Saisai, YU Haiyan*, WANG Junhua
College of Mechanical Engineering, Donghua University, Shanghai 201620, China

Abstract: To address the high cost of online detection equipment and the low adaptability and accuracy of online detection models that are caused by uneven lighting, high noise, low contrast and so on, a block-based template matching method incorporating fabric texture characteristics is proposed. Firstly, the template image set is evenly divided into *N* groups of sub-templates at the same positions to mitigate the effects of image illumination, reduce the model computation, and enhance the detection speed, with all image blocks being preprocessed. Then, the feature value information is extracted from the processed set of sub-templates at the same position, extracting two gray-level co-occurrence matrix (GLCM) feature values for each image block. These two feature values are then fused to construct a matching template. The mean feature value of all image blocks at the same position is calculated and used as the threshold for template detection, enabling automatic selection of template thresholds for different positions. Finally, the feature values of the image blocks in the experimental set are traversed and matched with sub-templates at the same positions to obtain fabric defect detection results. The detection experiments are conducted on a platform that simulates a fabric weaving environment, using defective gray fabrics from a weaving factory as the detected objects. The outcomes demonstrate the efficacy of the proposed method in detecting defects in gray fabrics, the mitigation of the impact of uneven external lighting on detection outcomes, and the enhancement of detection accuracy and adaptability.

Keywords: defect detection; gray-level co-occurrence matrix (GLCM); template matching; gray fabric; feature extraction; online detection
CLC number: TP391.41; TS101.9 **Document code**: A
Article ID: 1672-5220(2025)06-0594-12

Open Science Identity (OSID)

0 Introduction

In the textile industry, factors, including machine malfunctions, yarn breaks and improper manual operations, could result in various types of fabric defects, thereby causing significant economic losses for textile companies[1-2]. At present, defect detection in textiles mainly relies on manual detection. Statistics show that the error rate of manual detection is generally 35%–55%[3]. When the fabric width exceeds 2 m and the detection speed is higher than 30 m/min, the missed detection rate can reach as high as 60%[4-5]. Two types of commercially available automated fabric detection systems for the domestic and international textile industry are online detection and offline detection[6]. Although offline automated fabric detection systems can improve the detection efficiency, their high cost limits widespread adoption[7]. Online automated fabric detection systems integrated into weaving machines offer several advantages, including the elimination of the need for detection workshops and the provision of real-time feedback on the fabric quality[8]. However, due to constraints such as the weaving workshop environment, installation space and system cost, online automated fabric detection systems face challenges in detecting defects under conditions of uneven lighting, high noise and low contrast[9]. The improvement of the detection accuracy and algorithm adaptability under these conditions remains a critical issue.

Currently, some methods are relatively mature in the detection of fabric defects. Mak et al.[10] proposed a real-time computer vision system for detecting defects in fabrics, enabling online defect detection. This system detects defects by automatically tuning the Gabor functions to match the texture information. Schneider et al.[11] introduced a high-precision online fabric defect detection system integrated with the loom machinery and software. However, these two online detection systems have certain issues: they have high requirements for the image quality and are heavily reliant on advanced hardware equipment. Furthermore, they rarely consider addressing related problems, such as uneven lighting, through software upgrades. Consequently, these factors lead to high detection costs and low accuracy when handling fabrics in varying widths.

Template matching is one of the key technologies in the field of computer vision. Its basic principle involves the comparison of the similarity between a template image and the target image, thus offering advantages such as simplicity and high accuracy. Template matching has found widespread application in the target recognition on

Received date: 2024-11-18
* Correspondence should be addressed to YU Haiyan, email: yuhy@dhu.edu.cn
Citation: LI S S, YU H Y, WANG J H. Gray fabric defect detection based on statistical template matching[J]. *Journal of Donghua University (English Edition)*, 2025, 42(6): 594-605.

regular surfaces (such as metals), workpiece positioning and object tracking[12]. Shi et al.[13] developed a monitoring system for a stamping material collection line that utilized vision-based non-contact detection technology in conjunction with artificial intelligence (AI) image algorithms. This system autonomously executes template matching with reference images, facilitating real-time online monitoring of diverse regions of the drawing components amid strong vibrations and complex lighting conditions. Wang et al.[14] proposed a real-time online template matching method which focused on edge features, improving the matching accuracy and effectively overcoming disturbances such as lighting and occlusion. However, woven fabrics, composed of interwoven warp and weft yarns, possess complex surface characteristics that cannot be effectively handled by conventional template matching methods for defect detection. The gray-level co-occurrence matrix (GLCM), a classical method in the texture analysis, identifies defects by assessing the disruption of statistical texture features. Its application in fabric defect detection has been extensive. Hamdi et al.[15] utilized the GLCM to calculate the Euclidean distance between each GLCM and a reference matrix. They then compared the distances to pre-determined thresholds, achieving a high detection accuracy. Gustian et al.[16] combined the GLCM with the principal component analysis for feature extraction and used multi-class support vector machines with Gaussian kernels or radial basis functions for classification, thereby enhancing the algorithm's recognition precision. However, the diverse defect characteristics of fabrics make it challenging to directly identify defects based solely on statistical texture features.

The traditional statistical-based fabric detection methods have a low success rate in detecting fabrics with inconspicuous textures or fine structures. Moreover, the computational process is time-consuming due to the large volume of data[17]. While deep learning methods offer a high accuracy, they necessitate tens of thousands of samples for training, rendering the collection process in factory environments labor-intensive and time-consuming. Although defect generalization methods can increase the sample size, the discrepancies between generated samples and actual factory defects often result in suboptimal detection performance. Furthermore, deep learning methods are highly reliant on complex hardware systems[18-19]. In comparison to these approaches, the method proposed in this paper requires only a few hundred images to generate templates, significantly reducing both the required sample size and computational resources.

Based on the preceding analysis, this study aims to propose a novel real-time online detection method that integrates the strengths of the template matching for real-time online detection and GLCM for texture feature description. Experimental validation on industrial fabric samples reveals that the proposed method attains a higher detection accuracy and better adaptability, particularly in challenging conditions such as uneven lighting, high noise and low contrast, while fulfilling the requirements for online detection.

1 Design Principles and Framework

The statistical template matching method is predicated on the utilization of feature values derived from the GLCM obtained from blocks at the same positions to construct matching templates. This methodology enables the algorithm to effectively capture essential characteristics of fabric textures and defects. The matching process entails a comparison of the feature values of experimental images with those of the established templates. To enhance adaptability, the method partitions the template set into sub-templates, creating smaller templates for various positions and facilitating image matching within the same region. This strategy mitigates issues such as uneven lighting across different areas caused by variations in illumination and weaving processes. Furthermore, the method automatically determines the threshold for sub-templates by calculating the mean of the feature values, thus eliminating the need for manual adjustments based on prior experience.

The framework of the proposed method is illustrated in Fig. 1 and comprises the following steps.

1) Dataset classification. The captured fabric images are divided into two groups: a non-defective template set and a defective experimental set.

2) Image cropping and block division. The fabric images are uniformly cropped and divided into smaller blocks, splitting each image into N groups of sub-templates (X_1, X_2, $\cdots$, X_N), where N denotes the total number of sub-templates.

3) Image preprocessing. The cropped and divided fabric images undergo histogram equalization and gray-level compression processing.

4) Feature extraction and template creation. By utilizing Haralick's feature extraction method[20], the feature values of K sub-image blocks X_i at corresponding positions within the template set are computed. These feature values are then fused across N groups of blocks at the same positions to create N matching templates.

5) Template matching. By using the N matching templates, the feature values of each sub-block in the experimental set images are traversed and matched with the corresponding templates. Defective samples are identified, and the image is classified as defective or non-defective based on the presence of marked defects.

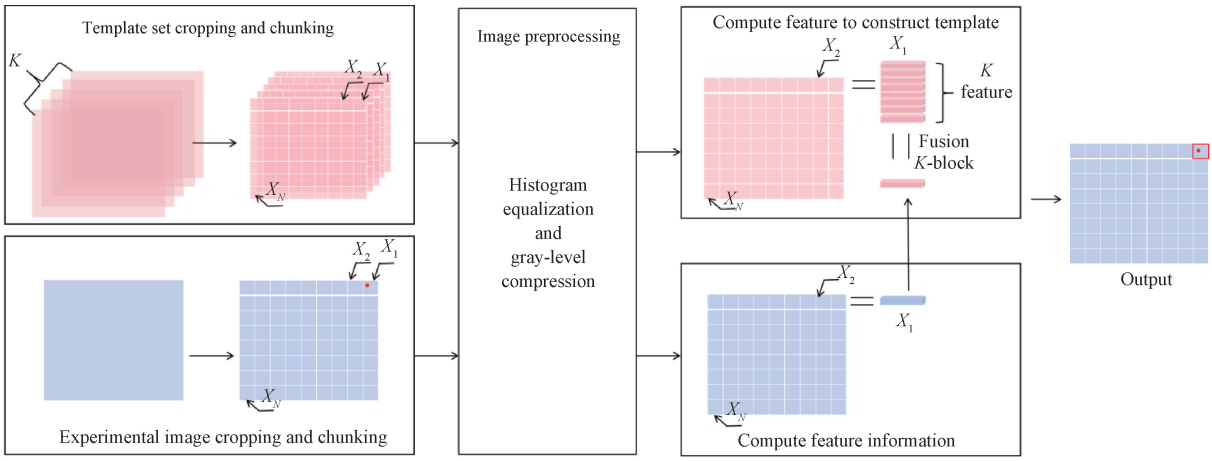

Fig. 1 Framework of fabric defect detection

2 Fabric Defect Detection Method

2.1 Image cropping and block division

In fabric defect detection, images captured by industrial cameras are frequently influenced by the harsh factory environment, resulting in uneven lighting conditions and low image resolution. The direct utilization of statistical GLCM feature values for the construction of matching templates significantly increases the computational load during feature value calculation. This poses a significant challenge in meeting the real-time detection requirements of factory applications. Furthermore, the low quality of the captured images has a detrimental effect on the accuracy of the template matching process. To address these issues, this study employs an image block processing approach. The fabric image is divided into N small square blocks, and the feature values of each block are calculated independently. This approach effectively reduces the computational burden and establishes a foundation for real-time template matching. Furthermore, the employment of block processing facilitates the calculation of localized feature statistics, thereby mitigating the impact of uneven lighting across the entire fabric image. If the captured image is $m \times m$ pixels and each small block is $p \times p$ pixels, the number of blocks N can be expressed as

$$N = (m/p) \times (n/p). \quad (1)$$

The proposed algorithm utilizes a sub-block as a template, with the sub-block size being a critical parameter that exerts a direct influence on the detection performance. The image size employed in this study is 2 592 × 1 944 pixels. If the sub-block is of insufficient size, it may fail to capture the complete fabric texture information, although it can better highlight defects. Conversely, if the sub-block is too large, it captures more comprehensive fabric texture information, but the relative proportion of defective areas within the sub-block decreases, adversely affecting the detection accuracy. For gray fabric production, it is a common occurrence for small cottonseed shells to be present on the fabric surface as a normal feature. To avoid the misclassification of these defects while ensuring the maximization of defect information retention, a sub-block size of 75 × 75 pixels was selected. This size strikes a balance between capturing sufficient texture details and minimizing false detections. Before creating matching templates, it is necessary to crop excess pixels from the image edges to ensure uniform dimensions across all images. For unknown fabric types, where defect sizes and distribution patterns are unpredictable, defects may otherwise fall between sub-blocks or be cropped out at the edges, as illustrated in Fig. 2. To address this issue, a multi-position block cutting method is designed. This method involves the shifting of the cropping region in five directions: top left, bottom left, bottom right, top right and center, as illustrated in Fig. 3. The application of multi-position cropping to the template set results in the generation of 850 sub-block templates for each position, thereby yielding templates for five distinct positions. A similar approach is adopted for the experimental set, where multi-position cropping and block processing are first applied to generate five positional images of experimental sub-blocks, and then each block is matched to the template at the corresponding positions.

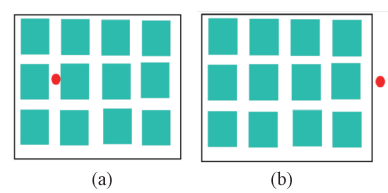

Fig. 2 Special position defects: (a) defects between sub-blocks; (b) defects at cropped edge

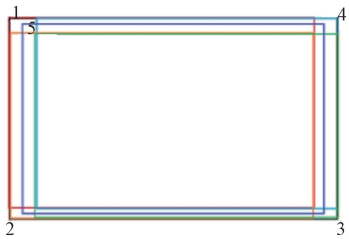

Fig. 3 Multi-position block cropping method

2.2 Preprocessing of fabric images

The background texture of woven fabrics exhibits periodic and regular characteristics, which can severely interfere with defect detection and classification. Image enhancement techniques are employed to suppress noise from the background texture. Histogram equalization is employed to adjust the grayscale distribution of the image, thereby ensuring more uniform distribution of the grayscale levels. This enhances both image contrast and overall quality, thereby improving the effectiveness of defect detection[21]. Histogram equalization is a widely adopted technique for fabric texture denoising and enhancing contrast. It operates by transforming the image's cumulative distribution function (CDF), which is derived from the frequency values of each grayscale level in the histogram. Here, the frequency value represents the number of pixels in the image at a specific grayscale level. By mapping the original pixel values to new equalized values based on the CDF, a histogram-equalized image is produced. The process enhances image contrast and minimizes interference from periodic fabric textures. The calculation is

$$C(v)=\text{round}((L-1)\times C_1(v)), \tag{2}$$

where $C(v)$ is the equalized grayscale level; L is the number of grayscale levels in the image, typically 256; $C_1(v)$ is the value of the CDF at a grayscale level of v in the original image.

Histogram equalization is performed on both defect-free and cotton ball defect images after block division, as described by Eq. (2). The visual comparison of images before and after histogram equalization is presented in Fig. 4. It is evident that histogram equalization improves the clarity of fabric images by suppressing background texture noise while enhancing the texture features in both normal and defective regions.

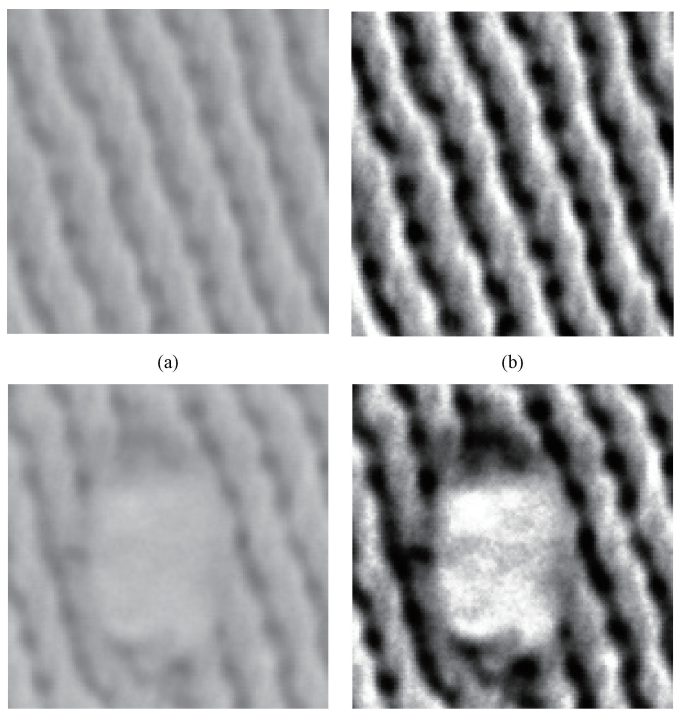

Fig. 4 Histogram-equalized images: (a) defect-free image; (b) defect-free image after histogram equalization; (c) cotton ball defect image; (d) cotton ball defect image after histogram equalization

Typically, after histogram equalization, the matrix gray levels of an image are distributed in 0–255. The computational complexity of the GLCM is determined by both the image's grayscale levels and its size. Directly calculating the GLCM for images with 0–255 gray levels results in an excessive computational load and high resource usage[22]. Therefore, the compression of the image's gray level is required. Normally, gray levels are compressed to 8, 16 or 32. Using too low gray levels may compromise the fabric's texture structure, while using too high gray levels may slow down the algorithm's computation speed. To balance the reduction in

computational complexity with maintaining the image accuracy, the gray levels of fabric images are compressed to 16.

2.3 Feature extraction

The GLCM is an effective method for describing image texture information. It uses a matrix based on the gray level and the relative position relationship between pixel pairs, recording the frequency of occurrences of gray level combinations of adjacent pixels at specific directions and distances in the image[23-24]. After gray-level compression, as shown in Fig. 5(a), for each pair of pixels (i, j) in the compressed image, pixel pairs with a specific distance d and direction θ are identified. The frequency at which this pair of grayscale values appear is counted, and this count represents the pixel value $A(i, j)$ in the GLCM. The size of the GLCM corresponds to the number of compressed grayscale levels. For $d=1$ and $\theta=0$, the GLCM computed from the image in Fig. 5(a) is shown in Fig. 5(b).

1	1	9	11	16
4	5	9	14	2
7	9	14	1	3
16	9	1	3	10

(a)

	1	2	3	4	5	6	7	8	9	10	11	12	13	14	15	16
1	1	0	2	0	0	0	0	0	0	0	0	0	0	0	0	0
2	0	0	0	0	0	0	0	0	0	0	0	0	0	0	0	0
3	0	0	0	0	0	0	0	0	0	1	0	0	0	0	0	0
4	0	0	0	0	1	0	0	0	0	0	0	0	0	0	0	0
5	0	0	0	0	0	0	0	0	1	0	0	0	0	0	0	0
6	0	0	0	0	0	0	0	0	0	0	0	0	0	0	0	0
7	0	0	0	0	0	0	0	0	1	0	0	0	0	0	0	0
8	0	0	0	0	0	0	0	0	0	0	0	0	0	0	0	0
9	1	0	0	0	0	0	0	0	0	0	1	0	0	2	0	0
10	0	0	0	0	0	0	0	0	0	0	0	0	0	0	0	0
11	0	0	0	0	0	0	0	0	0	0	0	0	0	0	0	0
12	0	0	0	0	0	0	0	0	0	0	0	0	0	0	0	1
13	0	0	0	0	0	0	0	0	0	0	0	0	0	0	0	0
14	1	1	0	0	0	0	0	0	0	0	0	0	0	0	0	0
15	0	0	0	0	0	0	0	0	0	0	0	0	0	0	0	0
16	0	0	0	0	0	0	0	0	1	0	0	0	0	0	0	0

(b)

Fig. 5 GLCM with $d=1$ and $\theta=0$: (a) grayscale levels; (b) GLCM corresponding to 16 gray levels

The selection of the step size and direction parameters of the GLCM is very important. A large step size leads to the weakening of local texture features, which affects the detection accuracy, while a small step size captures local texture information, which is important for the detection of small or fine blemishes. Therefore, a step size of one pixel is employed to ensure the accurate capture of texture features. We extracted symbiotic matrix features in four directions (0°, 45°, 90° and 135°), each of which can yield different feature values, which is too complex to represent texture features, so the feature values obtained in these four directions are averaged as the window feature values. This setup aims to minimize the influence of directional textures on the feature extraction results.

The GLCM cannot describe texture features directly. In this research, two statistical features (energy and entropy) of the GLCM are calculated to represent the texture features of the image block X_i. Energy reflects the uniformity of the grayscale distribution in the image, whereas entropy quantifies the quantity of information in the image and reflects the degree of textural non-uniformity. Energy and entropy feature values are computed as

$$G = \sum_{i=0}^{N_g-1} \sum_{j=0}^{N_g-1} (P(i, j))^2, \tag{3}$$

$$T = -\sum_{i=0}^{N_g-1} \sum_{j=0}^{N_g-1} P(i, j) \ln P(i, j), \tag{4}$$

where G and T are the energy and entropy feature values, respectively; $P(i, j)$ is the value at the ith row and jth column of the GLCM; N_g is the number of compressed grayscale levels.

The energy and entropy feature values of the image block X_i are computed by using Eqs. (3) and (4), specifically for subtle defect types such as broken warp and small cotton ball defects. The findings are displayed in Fig. 6. Broken warp defects appear in column 21 of the image, as shown in Fig. 6(b). The feature values of column 21 are represented by the red dots after the feature values have been arranged, as shown in Figs. 6(c) and 6(d). Cotton ball defects are in row 10 and column 25 of the image, as shown in Fig. 6(f). After feature sorting, the feature values of these rows and columns are represented by the red dots, as shown in Figs. 6(g) and 6(h). Compared to cotton balls and broken warps, other types of defects are more noticeable in terms of the size and characteristics. Therefore, the energy and entropy feature values of the image block X_i are used as template matching metrics to effectively separate defective image blocks.

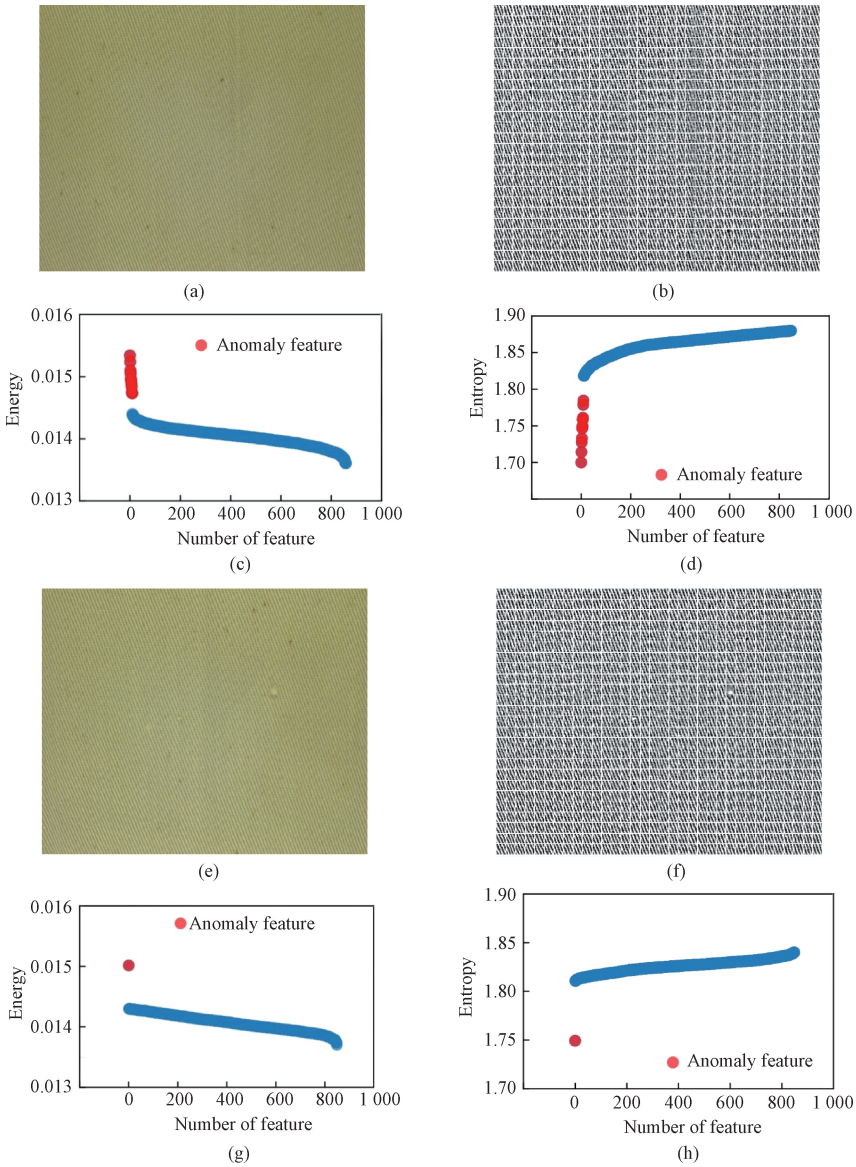

Fig. 6 Analysis of image characteristics of broken warp and cotton ball with inconspicuous defects: (a) original image of broken warp; (b) histogram equalization of broken warp after image blocking; (c) energy feature map of broken warp; (d) entropy feature map of broken warp; (e) original image of cotton ball; (f) histogram equalization of cotton ball after image blocking; (g) energy feature map of cotton ball; (h) entropy feature map of cotton ball

2.4 Template creation

Based on the above analysis, the feature values of the defective blocks are larger than those of normal texture blocks, while the feature values of the normal texture blocks exhibit smaller variations. Due to the large size of the captured image (2 592 × 1 944 pixels), there are differences in the light intensity at different positions, causing the feature values of normal texture blocks to have smaller variations. To mitigate this effect, the concept of chunked template matching is proposed.

N sets of distinct feature values are generated by calculating the feature values of each block X_i at each position after the fabric template set has undergone block division and preprocessing. Multiple matching templates are created for various positions within the template set to minimize the variation in feature values between regions. Figure 7 displays the feature value information for each block X_i at each position in the template set. The feature values follow a Gaussian distribution, with most values distributed around the mean, which helps to summarize the center of the template the most effectively. The feature values of all blocks X_i at the same position in the template set are used to describe the regional texture information. To ensure template invariance, the computed mean of the feature values for all blocks X_i at the same position is statistically used to automatically generate the template threshold for that position.

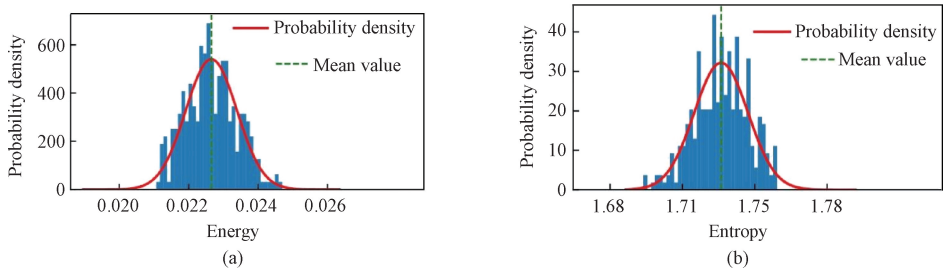

Fig. 7 Energy and entropy Gaussian distribution of block images at the same position: (a) probability distribution of energy feature values; (b) probability distribution of entropy feature values

Template information typically consists of all feature data from the template image. To fully exploit the image features, this study creates a multidimensional Gaussian feature template by using the feature values of all blocks at the same position in the template set. In this process, a one-dimensional Gaussian distribution is extended to a two-dimensional Gaussian distribution to improve the template-matching relationship. Firstly, extract two texture feature values, energy and entropy, from all blocks at the same position in the fabric template set. Secondly, integrate these feature values from all blocks to construct the matching template information. The resulting three-dimensional Gaussian distribution probability density function is shown in Fig. 8(a), and Fig. 8(b) presents the contour plot of Fig. 8(a) on a two-dimensional plane. Then, in the feature space, find an optimal feature curve based on the Gaussian distribution contours to form the feature-matching template, ensuring that the entire or most template samples are contained within the curve. Finally, match the feature values with the feature template.

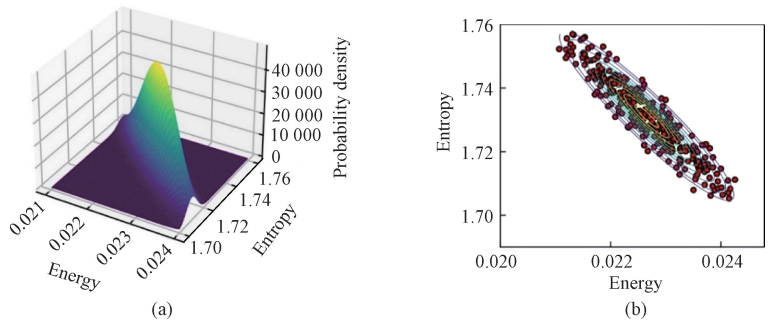

Fig. 8 Same position of match templates: (a) Gaussian template; (b) contour plot

Given a target image block X_i, let G_i and T_i represent the feature values for energy and entropy of the target image block, where $i = 1, 2, \cdots, N$ ($N = 850$, five groups in total) and i indicates different position blocks. There is a significant difference in the feature values between normal and abnormal texture regions in the fabric. The mean feature values of all image blocks X_i at the same position in the template are used as the threshold for calculating the image template match. The offset of the feature values of the target image block X_i relative to the threshold is used as the descriptor. If the feature values of the target image block fall within the defined feature curve, the sample is considered similar to the template and is classified as a normal point. Conversely, if the feature values do not match the template, the sample is classified as an abnormal point. The result of the template matching is

$$P_i = \begin{cases} |G_i - \mu_i| > k_0 \times \mu_i, \\ |T_i - \mu_j| > k_1 \times \mu_j, \end{cases} \tag{5}$$

where P_i is the matching result; μ_i and μ_j are the mean values of the energy and entropy feature values for all image blocks X_i at the same position in the template, respectively; k_0 and k_1 are the ratio thresholds for the template. The detection results for different values of k_0 and k_1 are shown in Table 1.

Table 1 Detection results for different ratio thresholds

Ratio threshold		Correct detection rate P_c/%	False detection rate P_f/%
k_0	k_1		
0.02	0.02	100	21.2
0.02	0.03	100	19.0
0.03	0.02	96.5	18.5
0.03	0.03	93.9	9.0
0.03	0.04	89.6	7.4
0.04	0.03	89.0	4.3
0.04	0.04	87.3	4.3

A ratio threshold of 0.03 leads to a high correct detection rate and a reasonably low false detection rate. The highest correct detection rate and the highest false

detection rate are observed when the ratio thresholds are set at 0.02. The lowest rates of correct detection and false detection occur when the ratio thresholds are set at 0.04. After comparing the false detection rate and the correct detection rate, k_0 and k_1 are selected at 0.03 to improve the ability to identify the defective area.

3 Experimental Results and Analyses

3.1 Experimental test

To validate the effectiveness of the method, a fabric defect visual detection experimental system was set up, as shown in Fig. 9.

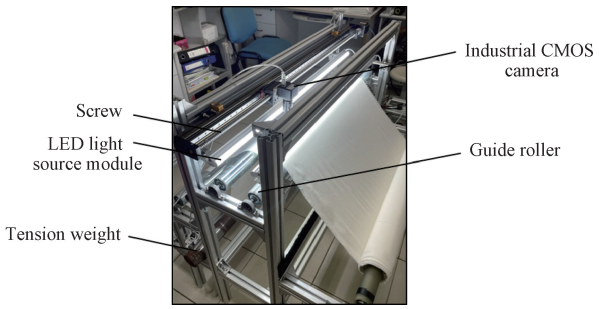

Fig. 9 Image detection experimental system

This replicates the operational environment of real-time detection. The hardware system is composed of two major modules: the motion control module and the image capture module. With the fabric feeding speed of 0.2 m/min in the weaving process, the servo motor does not need a high speed. The planetary reducer motor at the maximum speed of 125 r/min could meet the requirements of the longitudinal feeding movement. The motion control module utilizes the servo motor as the driving unit. The longitudinal feeding of the fabric on the equipment platform is completed by driving the coordinated operation of the rollers for rolling the fabric and the rollers for feeding the fabric. Tension weights, positioned between the guide rollers, assist in tensioning and balancing the fabric by utilizing the weights' gravitational force. The image capture module utilizes a 2 592×1 944 pixel CMOS area scan camera (Maishiv Technology Co., Ltd., China) and transmits data via a Gigabit Ethernet network interface. Since the feeding speed of the weaving equipment is lower than 0.03 m/min, the use of a mobile camera for image capture can effectively reduce the cost of the detection experimental system[25]. The light emitting diode (LED) is selected as the light source for the system.

In the experimental setup, the camera moves laterally by being mounted on a moving ball-screw slide, covering the full width of the fabric. The fabric width is 1 000.0 mm, and the simulated fabric feeding speed is set at 0.2 m/min. The working distance between the camera and the fabric is fixed at 250.5 mm, resulting in a camera's view field of 334.0 mm × 250.5 mm. Given the width of the view field of 334.0 mm, to ensure that all areas of the fabric are captured completely and unobtrusively, transverse shots are taken over a round-trip movement in 24 s, and five images need to be captured. Figure 10 shows an illustration of the visual coverage of the fabric as realized in the proposed detection system. In a single imaging cycle, the fabric moves 80.0 mm in the y-direction, and there is an overlap in the captured images, ensuring that all areas of the fabric are thoroughly captured horizontally and vertically without missing anything.

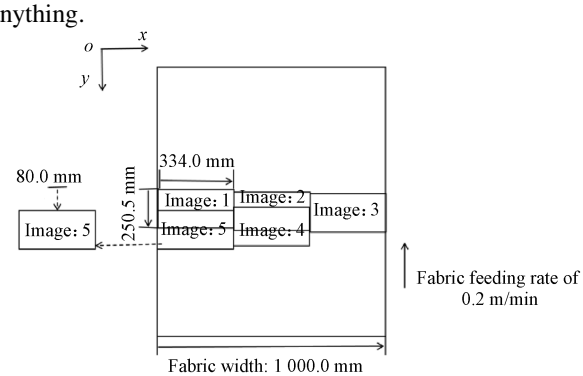

Fig. 10 Scheme of image capture module

The image capture module employs a low-cost CMOS camera. The images of the fabric collected under simulated factory lighting conditions exhibit poor quality and low resolution. Statistical analyses are conducted on the image quality collected in the simulated weaving environment, as shown in Fig. 11.

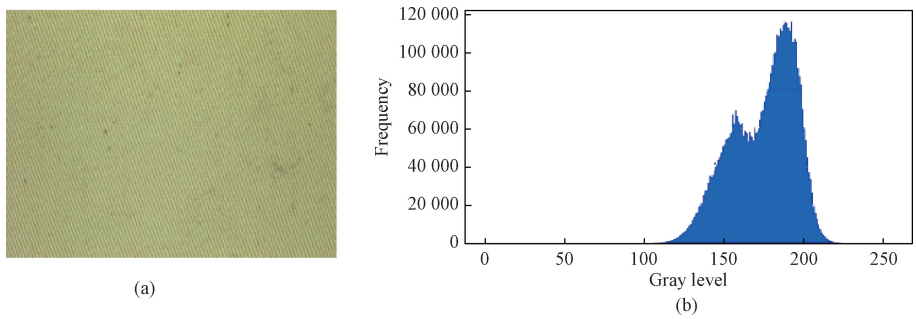

Fig. 11 Image light distribution: (a) original image; (b) grayscale histogram of original image

A thorough analysis of the grayscale histogram of the collected fabric image reveals a distribution that is concentrated in the middle-right region of the image, exhibiting two distinct peaks. This indicates the presence of two main grayscale values in the image, corresponding to shadowed and bright areas, which are attributable to variations in lighting conditions. The image also demonstrates a certain degree of contrast, and it is evident that the overall quality of the collected images is relatively low. However, the uneven lighting phenomenon shows a consistent pattern during the collection process, with the center appearing brighter and the edges darker. To address this issue, the block-based template creation method proposed in this paper involves generating templates for regions under the same lighting conditions. Concurrently, the corresponding regions of the experimental image are matched with the templates, thereby effectively resolving the problem of low-quality images caused by uneven lighting.

Fabric defects are categorized into more than 30 types, and the fabric utilized in the experiments of this paper is generated by the actual production process in the factory[26]. The experimental system involves the capture of 806 images (308 defect-free template images, 357 defect images and 141 defect-free test images). The software system for the detection method in this study incorporates an AMD Ryzen 75800U processor (2 GHz and 16 GB), with programming conducted in C++ on Visual Studio 2019.

3.2 Evaluation metrics and comparison results

To evaluate the performance of the defect detection method, two metrics are utilized: P_c and P_f. P_c is a measure of the system's capacity to correctly identify positive samples, while P_f is a proportion of negative samples that are erroneously classified as positive samples by the detection system. P_c and P_f can be calculated as

$$P_c = N_{tp}/(N_{tp} + N_{fn}), \tag{6}$$

$$P_f = N_{fp}/(N_{fp} + N_{tn}), \tag{7}$$

where N_{tp} represents the number of defective test samples correctly identified as defective; N_{fp} represents the number of non-defective test samples incorrectly identified as defective; N_{fn} represents the number of defective test samples that are not detected as defective; N_{tn} represents the number of non-defective test samples correctly identified as non-defective.

The experimental fabric from this study was utilized as a control to compare with current classical and state-of-the-art fabric defect detection methods, to validate the accuracy and adaptability of the proposed algorithm. For the fabric defect detection method based on GLCM features, a 5 × 5 sliding window was used to compute entropy in four directions[27]. The means of these four directional feature values was taken as the value for the center of the sliding window, resulting in a feature map. The defect detection method based on the Itti saliency model utilized down-sampling pyramids and Gabor filters to obtain brightness and orientation features[28]. These features were then normalized to produce a fabric defect saliency map. The most common defects in fabrics produced by the textile factory include broken warps, broken wefts, cotton balls and so on. The results of experiments on these defects are shown in Table 2 and Fig. 12.

Table 2 Results for different defect detection methods

Method	Type	Number	Correct number	False number	P_c/%	Overall P_c/%	Overall P_f/%
Ours	Broken warps	57	57	0	100	93.9	9.0
	Broken wefts	60	60	0	100		
	Cotton balls	111	93	0	83.8		
	Broken holes	69	69	0	100		
	Normal	141	128	13	91.0		
Ref. [27]	Broken warps	57	45	0	78.9	85.1	14.9
	Broken wefts	60	50	0	83.3		
	Cotton balls	111	89	0	80.1		
	Broken holes	69	69	0	100		
	Normal	141	120	21	85.1		
Ref. [28]	Broken warps	57	48	0	84.2	86.5	17.0
	Broken wefts	60	53	0	88.3		
	Cotton balls	111	87	0	78.4		
	Broken holes	69	69	0	100		
	Normal	141	117	24	83.0		

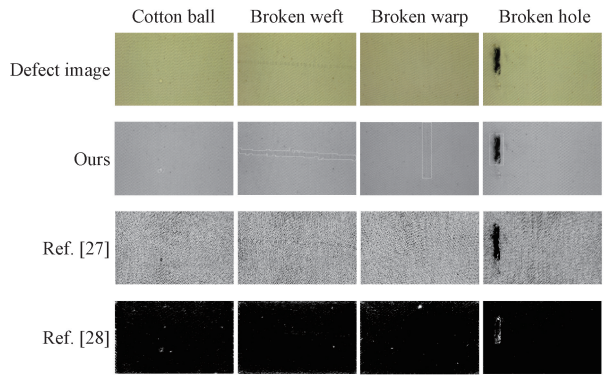

Fig. 12 Defect detection results in different types of fabrics

Current fabric defect detection methods generally achieve a P_c of approximately 80%–90% for warp defects in fabrics[29]. As shown in Table 2, the proposed method achieves a P_c of 100% in detecting defects such as broken warps, wefts and holes. In contrast, the other methods demonstrate a lower P_c for all defects except broken holes.

The cotton ball detection is a challenging task due to several factors: the size of cotton balls varies significantly (from a few millimeters to several centimeters), the color of cotton balls is like that of the fabric, and distinguishing between small cotton balls and cottonseed shells is difficult. The primary issues in detection are the false positives, where cottonseed shells are erroneously identified as cotton balls, and the failure to detect genuine cotton balls. However, the current fabric defect detection methods have less research on cotton ball defects and cottonseed shells, and cotton ball defects are the current difficulty in detection[30]. Images obtained in weaving environments, with issues such as uneven lighting, further reduce the contrast of cotton ball features, increasing the detection difficulty. The proposed method achieves a P_c of 83.8% for cotton balls, which is higher than that of other comparative methods.

The method in Ref. [27] employs the GLCM to directly compute feature values across the entire image, which results in longer processing time and more difficulties in meeting real-time detection requirements. Additionally, the texture differences between broken warps and normal textures are minimal, resulting in poor feature map display. The method in Ref. [28] employs the Gabor filtering to process the entire image, which makes some cottonseed shell features more prominent, consequently leading to a higher false detection rate. Furthermore, the low-contrast detection images frequently contain numerous bright spots in the periphery, which affect the detection performance. In comparison to these two methods, the proposed method is less affected by cottonseed shells and uneven lighting.

The average time taken by the method in this paper to process an image is 1 463 ms, while the production speed of commercially available weaving equipment is generally within 0.03 m/min. Given the image capture range and a fabric width of 2 m, the automatic detection method's processing efficiency is estimated at 0.25 m/min, meeting the timeliness requirements for online detection.

4 Conclusions

Current online fabric defect detection methods primarily rely on expensive hardware facilities, which results in high costs. Moreover, these methods often neglect the challenges posed by uneven lighting and the resulting degradation in the image quality under factory conditions. To address these issues, this paper proposes an online fabric defect detection method based on statistical template matching. The proposed method integrates the statistical analysis with the template matching by leveraging the GLCM to extract features from localized image blocks. These features are fused into a multidimensional template, which is then used to match the feature values of the images being inspected.

The experimental results demonstrate the efficacy of the proposed method in capturing the texture information of fabrics. The method exhibits a robust detection performance, even under conditions of uneven lighting. The method achieves an overall accuracy that exceeds 93%, at an average processing time of 1 463 ms. Furthermore, the method functions without relying on complex hardware, thereby significantly reducing the cost of manual inspection and meeting the requirements for real-time defect detection. However, challenges persist, particularly in distinguishing between similar characteristics of cotton balls and cottonseeds. Further research is necessary to enhance the detection accuracy in these scenarios.

References

[1] HUANG Y Q, JING J F, WANG Z. Fabric defect segmentation method based on deep learning [J]. *IEEE Transactions on Instrumentation and Measurement*, 2021, 70: 1-15.

[2] YANG J C, WANG C G, JIANG B, et al. Visual perception enabled industry intelligence: state of the art, challenges and prospects [J]. *IEEE Transactions on Industrial Informatics*, 2021, 17(3): 2204-2219.

[3] TAJERIPOUR F, KABIR E, SHEIKHI A. Fabric defect detection using modified local binary patterns [J]. *EURASIP Journal on Advances in Signal Processing*, 2007, 2008(1): 783898.

[4] CHO C S, CHUNG B M, Park M J. Development of real-time vision-based fabric inspection system [J]. *IEEE Transactions on Industrial Electronics*, 2005, 52(4): 1073-1079.

[5] ZHU R H, XIN B J, DENG N, et al. Review of fabric defect detection based on computer vision [J]. *Journal of Donghua University (English Edition)*, 2023, 40(1): 18-26.
[6] LI W Y, CHENG L D. New progress of fabric defect detection based on computer vision and image processing [J]. *Journal of Textile Research*, 2014, 35(3): 158-164. (in Chinese)
[7] XU W F, DAI M H, ZHU D, et al. Application progress of machine vision in fabric defect detection[J]. *Cotton Textile Technology*, 2021, 49(4): 80-84. (in Chinese)
[8] SCHNEIDER D, HOLTERMANN T, MERHOF D. A traverse inspection system for high precision visual on-loom fabric defect detection [J]. *Machine Vision and Applications*, 2014, 25(6): 1585-1599.
[9] WU Y, GUO P Y, LIU Y P, et al. Fabric defect detection based on local texture image representation [J]. *Journal of Donghua University (Natural Science)*, 2023, 49(6): 73-79.
[10] MAK K L, PENG P, LAU H Y K. A real-time computer vision system for detecting defects in textile fabrics [C]//2005 IEEE International Conference on Industrial Technology. New York: IEEE, 2005: 469-474.
[11] SCHNEIDER D, HOLTERMANN T, NEUMANN F, et al. A vision based system for high precision online fabric defect detection [C]//2012 7th IEEE Conference on Industrial Electronics and Applications (ICIEA). New York: IEEE, 2012: 1494-1499.
[12] MA J Y, JIANG X Y, FAN A X, et al. Image matching from handcrafted to deep features: a survey [J]. *International Journal of Computer Vision*, 2021, 129(1): 23-79.
[13] SHI L, WANG J Y, SUN S W, et al. Development on monitoring system for stamping receiving line based on visual inspection technology[J]. *Forging & Stamping Technology*, 2023, 48(9): 184-189. (in Chinese)
[14] WANG S Y, QIAN G K, LI D, et al. Real-time template matching method for edge features[J]. *Journal of South China University of Technology (Natural Science Edition)*, 2023, 51(9): 1-10.
[15] HAMDI A A, SAYED M S, FOUAD M M, et al. Fully automated approach for patterned fabric defect detection [C]//2016 Fourth International Japan-Egypt Conference on Electronics, Communications and Computers (JEC-ECC). New York: IEEE, 2016: 48-51.
[16] GUSTIAN D A, ROHMAH N L, SHIDIK G F, et al. Classification of troso fabric using SVM-RBF multi-class method with GLCM and PCA feature extraction [C]//2019 International Seminar on Application for Technology of Information and Communication (iSemantic). New York: IEEE, 2019: 7-11.
[17] ZHAO Y, ZUO B Q. Analysis on application of machine vision in fabric defect detection [J]. *Computer Engineering and Applications*, 2020, 56(2): 11-17. (in Chinese)
[18] ZHAO S X, ZHANG J, WANG J L, et al. Fabric defect detection algorithm based on two-stage deep transfer learning [J]. *Journal of Mechanical Engineering*, 2021, 57(17): 86-97. (in Chinese)
[19] ZHENG Y T, WANG C Q, CHEN L L, et al. Research progress of fabric image processing methods based on convolutional neural network [J]. *Advanced Textile Technology*, 2022, 30(5): 1-11, 20. (in Chinese)
[20] YUAN L H, FU L, YANG Y, et al. Analysis of texture feature extracted by gray level co-occurrence matrix [J]. *Journal of Computer Applications*, 2009, 29(4): 1018-1021. (in Chinese)
[21] PIZER S M, AMBURN E P, AUSTIN J D, et al. Adaptive histogram equalization and its variations[J]. *Computer Vision, Graphics, and Image Processing*, 1987, 39(3): 355-368.
[22] DU X L, ZHANG W, GU B B, et al. GLCM-based adaptive block compressed sensing method for image[J]. *Computer Science*, 2018, 45(8): 277-282. (in Chinese)
[23] GAO C C, HUI X W. GLCM-based texture feature extraction [J]. *Computer Systems & Applications*, 2010, 19(6): 195-198. (in Chinese)
[24] WANG Z S, FAN G B. Texture recognition method of remote sensing landform image based on multi-scale semi-coupled convolutional sparse coding[J]. *Computer Measurement & Control*, 2024, 32(10): 284-290. (in Chinese)
[25] LI C Y, YU H Y. Defect detection of plaid fabric based on periodic segmentation template subtraction [J]. *Cotton Textile Technology*, 2023, 51(3): 22-29. (in Chinese)
[26] YE S T, YOU S Q, HAO C, et al. Fabric defect detection based on cascade RCNN and two step clustering method [J]. *Cotton Textile Technology*, 2022, 50(7): 24-29. (in Chinese)
[27] WU Z, LIU X X, ZHENG L X, et al. A fabric defect detection method based on gray level co-occurrence matrix feature image [J]. *Cyber Security and Data Governance*, 2015, 34(21): 47-50, 54. (in Chinese)
[28] YAN B C, PAN R R, ZHOU J, et al. Real-time detection of fabric defects based on use of improved Itti salient model [J]. *Journal of Textile Research*, 2023, 44(7): 95-102. (in Chinese)
[29] MEI S Q, XIAO Z, CHEN J, et al. Improved

YOLOv5s fabric defect detection algorithm based on the fusion of global attention mechanism and decoupling head [J]. *International Journal of Information Retrieval Research*, 2024, 14(1): 1-18.

[30] WANG B, LI M, LEI C L, et al. Research progress in fabric defect detection based on deep learning[J]. *Journal of Textile Research*, 2023, 44(1): 219-227. (in Chinese)

基于统计学模板匹配的坯布疵点检测方法

李赛赛，于海燕*，王骏骅

东华大学 机械工程学院，上海 201620

摘　要：为了应对在线检测设备成本高，以及织物采集过程中图像亮度不均、高噪声和低对比度等问题导致疵点检测模型的适应性和准确性低的挑战，提出了一种融合织物纹理特性的分块模板匹配在线检测方法。首先，将模板集均匀分为 N 组同位置小模板集，以减小图像光照影响、降低模型计算量、提高检测速度，同时对所有图像块进行预处理。其次，对处理后的同位置小模板集进行特征值信息提取，提取每块图像块的两个灰度共生矩阵（GLCM）特征值，并将这两个特征值融合以构建匹配模板，同时计算相同位置所有图像块特征值的均值，作为模板检测的阈值，可实现不同位置模板阈值的自动选取。最后，通过遍历实验集中图像块的特征值与对应位置的小模板进行匹配，得到织物检测的结果。以织造车间采集的有疵点坯布为检测对象，在模拟织造环境搭建的织物图像采集检测平台上进行检测实验。结果表明，该方法能够有效检测坯布织物缺陷，显著降低外界光照不均对检测结果的影响，提高疵点检测的准确性和适应性。

关键词：疵点检测；灰度共生矩阵；模板匹配；坯布；特征提取；在线检测